Using ^{137}Cs and ^{210}Pb$_{ex}$ to assess soil redistribution on slopes at different temporal scales

L. Gaspar[1*], A. Navas[1], D.E. Walling[2], J. Machín[1], J. Gómez Arozamena[3]

1 Department of Soil and Water, Estación Experimental de Aula Dei, CSIC. Apartado 13034, 50080 Zaragoza, Spain.

2 Department of Geography , University of Exeter, Exeter EX4 4RJ, UK.

3 Universidad de Cantabria, Avenida Cardenal Herrera Oria s/n, 39011 Santander, Spain.

[*]Corresponding author. Email: lgaspar@eead.csic.es

Abstract

Increasing risk of soil loss as a result of climate change, has generated a need for reliable information on erosion rates at different temporal scales. Use of the fallout radionuclides ^{137}Cs, ^{210}Pb$_{ex}$ and ^{7}Be as tracers of sediment mobilisation and redistribution makes it possible to obtain estimates of soil redistribution rates within both undisturbed and cultivated landscapes over a range of timescales. Mediterranean landscapes are characterized by a great diversity of physiography and land use, and as a consequence erosion and deposition patterns are highly variable spatially. To document such spatial variability, a slope transect located in the subhumid Pre-pyrenean mountains (NE Spain) was selected to use ^{137}Cs and ^{210}Pb$_{ex}$ to assess medium- and longer-term soil redistribution rates. A total of 23 sectioned soil cores spaced 50 m apart were collected along the slope transect, where ^{7}Be had been previously used to document soil redistribution resulting from an individual storm event. The inventories of both radionuclides varied markedly, between 409 and 6080 Bq m^{-2} for ^{137}Cs, and between 0 and 6734 Bq m^{-2} for ^{210}Pb$_{ex}$. Estimates of soil redistribution, derived from the ^{137}Cs depth profiles, using appropriate conversion models, show that erosion rates along the transect vary between 2.6 and 31.9 Mg ha^{-1} $year^{-1}$, and that sedimentation rates vary between 0.2 and 24.5 Mg ha^{-1} $year^{-1}$. The highest soil losses occur in cultivated fields, within the midslope zone of the transect, while the highest deposition rates are found in tilled fields within the lower part of the transect. Erosion rates from $^{210}Pb_{ex}$ varied widely between 0.1 and 83.7 Mg ha^{-1} $year^{-1}$ on the lower slope, whereas sedimentation rates ranged between 0.8 and 110 Mg ha^{-1} $year^{-1}$ also at the bottom slope. The spatial distribution of the radionuclides along the transect reflects the effects of different land use and slope gradient on water erosion. The results obtained confirm the potential for using ^{137}Cs and $^{210}Pb_{ex}$ measurements for assessing soil redistribution on slopes in the Mediterranean environment over different temporal scales.

Key words: fallout radionuclides; ^{137}Cs; $^{210}Pb_{ex}$; soil redistribution; timescales; Mediterranean environments.

1. Introduction

Soil erosion and sediment transport and deposition represent a serious problem throughout the world, because of their impact on sustainable agricultural production as well as on environmental conservation. Severe erosion may promote desertification, especially in semiarid environments that are common in Mediterranean regions (Sadiki et al., 2007).

The Mediterranean environment is characterized by a seasonal climate with irregular but frequent and intense rain events, low vegetation cover, and soils with a high stone content. Rainfed crops, such as cereals, cover large areas in the drier parts of Mediterranean countries and frequently occupy mountainous areas. An increase of extreme daily rainfall in spite of a decrease in total annual rainfall has been reported for

Spain in recent years (López-Moreno et al., 2009). Highly erosive rainfall on these sloping landscapes can result in severe erosion of cultivated land (López-Vicente et al., 2008). In northeastern Spain, agriculture developed intensively over the last centuries through widespread deforestation and subsequent land abandonment has led to increased runoff and soil erosion (Navas et al., 2009).

To tackle the environmental threat posed by the loss of productive soil, the quantification of soil erosion rates is a first requirement. Thus, for Europe, the current state of scientific knowledge indicates that tolerable soil erosion rates range from ca. 0.3 to 1.4 t ha^{-1} yr^{-1} (Verheijen et al., 2009). There are many limitations associated with traditional techniques for documenting rates of soil erosion and sediment redistribution. Isotopic techniques based on the use of fallout radionuclides "FRNs" such as ^{137}Cs, ^{7}Be and $^{210}Pb_{ex}$ (e.g. Zapata, 2002) have been increasingly applied over the past 20 years as a means of obtaining spatially distributed information on erosion and deposition rates. The advantages and limitations associated with the use of the individual radionuclides for assessing soil erosion has recently been reviewed by Mabit et al. (2008).

The potential for using caesium-137 to quantify medium-term (c.a 50 years) soil erosion rates under different agro-environmental and natural conditions has been successfully demonstrated in a wide range of environments in different regions of the world (Ritchie and Ritchie, 2007) including Spain (e.g. Navas and Walling, 1992; Quine et al., 1994; Schoorl et al., 2004; Navas et al., 2007). Naturally derived ^{210}Pb, arriving at the land surface as fallout is rapidly and firmly adsorbed by the surface soil and subsequently redistributed across the landscape in a manner similar to ^{137}Cs, offers potential for quantifying soil redistribution rates over a longer timescale than ^{137}Cs (ca. 100 years). Unlike ^{137}Cs, deposition of fallout ^{210}Pb from the atmosphere has been relatively constant through time because of its natural origin (Crickmore et al., 1990).

To date $^{210}Pb_{ex}$ has been applied successfully in diverse agricultural landscapes of the world (e.g. Walling et al., 1995, 2003; Walling and He, 1999; Wallbrink and Murray, 1996; He and Walling, 1997; Matisoff et al., 2002; Zhang et al., 2006). However, at present its potential as a tracer of soil erosion is less widely recognized than ^{137}Cs and there have to date been few attempts to compare erosion rates estimated using both ^{137}Cs and ^{210}Pb (Zhang et al., 2006; Porto et al., 2009; Kato et al, 2010). ^{7}Be is as a natural short-lived ($T_{1/2}$=53 days) fallout radionuclide of cosmogenic origin, that permits soil redistribution to be assessed for individual events or short periods of heavy rainfall (Walling et al., 1999; Schuller et al., 2006) and it has been applied successfully in Mediterranean environments (Navas et al., 2008). As with ^{137}Cs and $^{210}Pb_{ex}$ measurements, the estimation of short--term soil redistribution rates from ^{7}Be measurements is based on a comparison between the ^{7}Be inventories for individual sampling points and the local reference inventory.

Concern for the increasing risk of erosion under climate change in the Mediterranean region (Meehl et al., 2005) has emphasised the need for data on soil erosion rates at different temporal scales in order to quantify the potential changes that might occur and their impacts. Furthermore, important land use changes occurring during the past century that are recognized to have had clear impacts on soil redistribution (Navas et al., 2005) could be traced for different timescales using "FRNs".

Measurements of artificial ^{137}Cs and natural $^{210}Pb_{ex}$ inventories in the landscape can be used to obtain average soil redistribution rates integrating many years of erosion and deposition processes. In the case of ^{137}Cs, estimates of soil redistribution rates will extend from the commencement of ^{137}Cs fallout in the late 1950s to the present. In contrast, the continuous fallout of Pb result in $^{210}Pb_{ex}$ inventories sensitive to erosion and deposition occurring within a period equivalent to four times the half-life, i.e. the past 100 years, although the progressive reduction in the effect of past changes in the contemporary $^{210}Pb_{ex}$ inventory would mean that $^{210}Pb_{ex}$ inventory will be more sensitive to recent soil redistribution (Walling, 2003).

To date few studies have used $^{210}Pb_{ex}$ to derive information on soil erosion in Mediterranean landscapes (Porto et al., 2006, 2009). In Spain, preliminary research involving the combined use of both ^{137}Cs and $^{210}Pb_{ex}$ to assess soil redistribution has been undertaken in the Pyrenees (Navas et al., 2003). The potential of combining ^{137}Cs and $^{210}Pb_{ex}$ to document soil redistribution over different time scales needs further exploration, because at present little information exits on the use of this approach, especially in stony soils of mountain landscapes.

In this study, $^{210}Pb_{ex}$ is used in combination with ^{137}Cs to derive additional information on the pattern of soil redistribution along a mountain slope transect representative of rainfed agrosystems in mountain landscapes of the Pre-Pyrenean Range that includes different soil types, land use and slope gradients. Estimates of soil erosion and sedimentation rates have been derived using appropriate models (Walling and He, 1999; Soto and Navas, 2004, 2008). Soil redistribution estimates have also been compared with values derived from ^{7}Be measurements that were undertaken at the same location during a previous study (Navas et al., 2008) to compare the soil redistribution rates for the longer temporal scale provided by ^{137}Cs and $^{210}Pb_{ex}$ with those for an individual storm event derived from ^{7}Be measurements. This research aims to explore further the potential for combining ^{137}Cs and $^{210}Pb_{ex}$ measurements to document soil redistribution over different time scales in stony soils of Mediterranean rangeland and agricultural landscapes.

2. Materials and methods

2.1. Radionuclides as sediment tracers

Fallout ^{137}Cs (half-life 30.2 year) was introduced in the stratosphere as a result of thermonuclear weapons test, with fallout beginning in 1952 and continuing to the mid 1970s, with a peak in 1963, the year of the Nuclear Test Ban Treaty. Pb-210 is a natural product of the ^{238}U decay series derived from the decay of gaseous ^{222}Rn, the daughter of ^{226}Ra. ^{226}Ra is found naturally in most soils and rocks and will generate ^{210}Pb which will be in equilibrium with its parent. A small quantity of ^{222}Rn diffuses upwards from the soil and introduces ^{210}Pb into the atmosphere and provides an input of this radionuclide to surface soils and sediments which +is not in equilibrium with its parent ^{226}Ra. This fallout component is termed unsupported or excess ^{210}Pb ($^{210}Pb_{ex}$) when incorporated into soils in order to distinguish it from ^{210}Pb produced in situ by the decay of ^{226}Ra.

Like ^{137}Cs, $^{210}Pb_{ex}$ fallout will be rapidly adsorbed by the clay minerals and organic matter in the surface soil and its redistribution in the soil and across the land surface will occur in association with soil and sediment particles and will be primarily controlled by its interaction with land use practices, erosion and sediment transport processes (Walling and He, 1999), although some ^{137}Cs or $^{210}Pb_{ex}$ can be mobilized by chemical and biological processes.

Estimates of soil redistribution rates derived from ^{137}Cs and $^{210}Pb_{ex}$ measurements are based on a comparison of the total inventory for an individual sampling point and the local reference inventory. Where inventories are lower than the local reference inventory, the loss of radionuclide points to loss of soil. Similarly, inventories in excess of the reference level are indicative of addition of radionuclide and soil, by deposition. The magnitude and direction of the measured deviations from the local reference level provide a qualitative assessment of soil redistribution (Walling and Quine, 1990; Walling and He, 1999).

As indicated by Zhang et al. (2006) and unlike ^{137}Cs, the $^{210}Pb_{ex}$ inventory for a stable site can be assumed to be in steady state, with fallout inputs balanced by radioactive decay of the existing $^{210}Pb_{ex}$ inventory. For an eroding soil, loss of $^{210}Pb_{ex}$ through erosion will reduce the inventory, but the continuing fallout input introduces an important contrast with ^{137}Cs, for which fallout inputs effectively ceased in the 1970s, and for which inventories will progressively decline through time, even in the absence of erosion.

The redistribution rates based on $^{210}Pb_{ex}$ measurements have been estimated using the mass balance model developed by Walling and He (1999). The models reported by Soto and Navas (2004, 2008) for uncultivated and cultivated soils have been applied to estimate soil redistribution estimates based on ^{137}Cs measurements.

Statistical analysis was performed by one-way analysis of variance (ANOVA), and the means were subjected to a least-significant difference test (F test) to indicate the main differences in radionuclide activities and the soil redistribution rates derived from ^{137}Cs and $^{210}Pb_{ex}$ between the different parts of the transect. Pearson's linear correlations were also performed to find relationships between ^{137}Cs and $^{210}Pbex$ inventories and between the radionuclides and soil properties.

2.2. The study area

The study was conducted along a south facing slope transect located at the "Solá de Estaña" in the endorheic catchment of the Estaña lake (central part of the Pre-Pyrenees, NE Spain) (Fig. 1). The climate is continental Mediterranean, with an average annual rainfall of about 500 mm, distributed through the year to provide two wet periods, spring and autumn, and a dry summer with frequent high intensity rainfall events (López-Vicente et al., 2008). A 1250 m long transect extending from the catchment divide to the Estaña lake and with altitude ranging from 894 to 670 m was selected because is representative of mountain rainfed agrosystems in the region. Along the transect, the underlying parent material comprises Mesozoic strata, composed of limestone and clays with evaporite and gypsum deposits that correspond to the Muschelkalk and Keuper facies, respectively. A total of five types of soil have been identified along the transect. Calcisols and Leptosols, the predominant types, are associated with the limestones and Gypsisols, Regosols and Gleysols are associated with the clay materials.

Different land use, including natural forest, abandoned fields and cultivated fields, and different slope gradients are found along the transect. Agriculture commenced in the area several hundred years ago, occupying the lowland with gentle slopes surrounding the lake. Land use has since changed considerably, especially over the last two centuries. At the end of the 19th century demographic pressure caused an expansion of cultivation which transformed the rangeland slopes into agricultural land by constructing terraces and planting almond and olive trees as well as cereal crops. Subsequently land abandonment occurred during the 1950s as a result of major socio-economic changes in the 20th century that promoted migration to urban areas and abandonment of the less productive lands located on steep slopes. More recently under the European Agrarian Policy some of the steep marginal lands have been returned to cultivation.

2.3. Soil sampling and analyses

The soil sampling programme carried out along the Solá transect divided the transect into three parts, namely, the upper slope, midslope and bottom slope, to reflect the key contrasts in land use and slope gradient. Twenty four sampling points, each separated by 50 m, were located along the transect. Sampling point 13 was located on a thick Muschelkalk outcrop and a soil sample was not collected from this point. A total of 23 sectioned soil cores were therefore collected along the downslope transect. The upper slope with dense oak forest and a 24% slope provided 9 sectioned cores. The midslope with a mix of land use, including dense forest, scrubland, cultivated and abandoned land and an average slope of 21% provided 8 sectioned cores. The bottom slope, which has been cultivated for cereals over the last centuries has a 15% slope and was represented by 6 soil cores. In this section there is a pathway that interrupts the topographic profile of the slope between points 21 and 22 (Fig.1).

In order to characterize the depth distribution of $^{210}Pb_{ex}$ and ^{137}Cs, the soil cores were sampled at 5 cm depth intervals, reaching a maximum value of 55 cm in depth. Due to the abundance of stones that caused difficulties when sectioning the cores, some depth increments were 10 and 15 cm thick and in some cases the increments were less than 5 cm. At some points the maximum depth did not extend below 10 cm, although this situation was restricted to the Leptosols. The reference cores were collected from level undisturbed sites with a mature and natural vegetation cover that protects the soil surface from erosion.

Soil samples were collected using an 8 cm diameter automatic core driller. Also a hand-operated corer was used in shallow soils. A total of 143 soil samples were air-dried, ground, homogenised and quartered and passed through a 2 mm sieve. The weight of the fractions was recorded and subsamples of less than 2 mm were prepared for analyses. For the radionuclide gamma assays 50 g subsamples were transferred into airtight plastic pots and sealed for a period of 30 days prior to assay, in order to achieve equilibrium between ^{226}Ra and its daughter ^{222}Rn.

The ^{137}Cs and $^{210}Pb_{ex}$ activities were measured using a high resolution, low background, low energy, hyperpure coaxial gamma-ray detector coupled to an amplifier and multichannel analyser. The detector had an efficiency of 20%, and a 1.86 keV resolution (shielded to reduce background), and was calibrated using standard samples in the same geometry as the measured samples.

Gamma emissions of ^{137}Cs (661.6 keV line), ^{210}Pb (46.5 keV line) and ^{226}Ra (351.9 keV line of ^{214}Pb), were measured on 143 sub-samples. Counting times were 30000 s for ^{137}Cs and 86000 – 105000 s for ^{210}Pb, and the analytical precision of the measurements was approximately ±8% and ± 14% (95% level of confidence), respectively. The unsupported or excess ^{210}Pb ($^{210}Pb_{ex}$) concentration was calculated by subtracting the ^{226}Ra-supported ^{210}Pb concentration from the total ^{210}Pb concentration. The content of ^{137}Cs and $^{210}Pb_{ex}$ in the soil sample may be expressed as a concentration or mass activity (Bq kg^{-1}) and as activity per unit area or the inventory (Bq m^{-2}).

The stone content, soil texture and organic matter were determined following standard techniques (CSIC, 1976). To quantify organic matter a Mettler Toledo titrimeter and electrode were used. Granulometric, analyses of the sand, silt and clay size fractions was undertaken using a Coulter laser granulometer. To remove the organic matter prior to grain size analysis, samples were disaggregated chemically using 10% H_20_2 heated to 80 ºC, stirred, and subjected to ultrasound to facilitate particle dispersion.

3. Results and discussion

The reference ^{137}Cs inventory for the study area is 1570 (±80) Bq m^{-2} and was established from nine cores collected from level and stable sites that were not affected by erosion or deposition. The reference inventory agrees with the values found in other areas with similar environmental conditions in Spain. A reference inventory of 1940 Bq m^{-2} has been reported for the southern part of Spain (Schoorl et al., 2004) and a value of 1900 Bq m^{-2} for the Las Bardenas steppe in the north (Navas and Walling, 1992; Quine et al., 1994). In areas of higher annual precipitation, such as the Pyrenees, inventories of 4000 Bq m^{-2} in the Central Pyrenees (Navas et al., 2005) and even 6911 Bq m^{-2} in the Oriental Pyrenees (Sanchez-Cabeza et al., 2007) have been found. The reference $^{210}Pb_{ex}$ inventory of 1943 (±78) Bq m^{-2} for the study site was established from three depth profiles collected from level stable areas with no evidence of erosion or deposition. The depth distributions of both ^{137}Cs and $^{210}Pb_{ex}$ in the reference profiles exhibit peak concentrations at the surface and decline following the typical pattern with an exponential decay distribution with depth.

To date, few values of $^{210}Pb_{ex}$ reference inventory or $^{210}Pb_{ex}$ fallout flux have been reported for Spain, and the availability of such information is very limited more generally. A reference inventory for $^{210}Pb_{ex}$ of 5170 Bq m^{-2} has been reported for Devon, UK (Walling and He, 1999) and a value of 5730 Bq m^{-2} was reported for a site in China (Zhang et al., 2006). In northern Spain, reported values range from 1044 to 7044 Bq m^{-2} for the Lerida Pyrenees and from 2048 to 8204 Bq m^{-2} for Palencia (Sanchez-Cabeza et al., 2007). Information of the annual $^{210}Pb_{ex}$ fallout deposition fluxes in different areas of the world (Liu et al., 2001) include values ranging from 23 to 367 Bq m^{-2} equivalent to inventories between 767 and 12233 Bq m^{-2}, respectively. Assuming that the $^{210}Pb_{ex}$ inventory in a soil reflects a steady state between input from the atmosphere and radioactive decay, the average annual atmospheric ^{210}Pb flux for the study site is 60.39 Bq m^{-2} yr^{-1}, calculated according to the equation by Sanchez-Cabeza, et al. (2007),

$$^{210}Pb_{flux}\ (Bq\ m^{-2}\ yr^{-1}) = \lambda\ (yr^{-1}) \times {}^{210}Pb_{ex}\ inventory\ (Bq\ m^{-2})$$

where λ is the ^{210}Pb decay constant.

The ^{137}Cs flux from global fallout varies according to latitude. In the study area, located at 41º N, the impact of the Chernobyl accident appears to be negligible although some Chernobyl-derived radiocaesium was detected in the air around Valencia (Ferrero et al., 1987) and on the Mediterranean coast (Molero et al., 1999).

The ^{137}Cs and $^{210}Pb_{ex}$ mass activities in the sectioned cores varied greatly and for all depth increments (n=143) ranged between nd and 83.1 (±10.2) with a mean value of 5.3 Bq kg^{-1} for ^{137}Cs and between nd and 55.0 (±9.4) with a mean of 6.1 Bq kg^{-1} for $^{210}Pb_{ex}$. The ^{137}Cs and $^{210}Pb_{ex}$ inventories for all depth increments ranged between 0.0 and 4029.0 (±529.8) with a mean of 291.5 Bq m^{-2} for ^{137}Cs and between 0.0 and 2335.6 (±475.3) with a mean of 329.6 Bq m^{-2} for $^{210}Pb_{ex}$.

The large range of variation of the mass activities and inventories of both radionuclides reflect the depth distribution of the samples involved as well as the erosional status of the sampling point (i.e. eroding or deposition site). Within the soil profile, the lowest values occur at the deeper layers and highest values at the soil surface. However, depleted levels are found in the upper layers of eroded sites and also some enriched levels are found at the soil surface due to deposition. Accumulation of ^{137}Cs was found in deeper layers at point 24 located on the margin of the Estaña lake, that corresponds to a lake sediment deposit. In Mediterranean environments, large variations in the spatial distribution of radionuclides due to local factors, including vegetation distribution, stoniness, topographic roughness, tillage and large variety of land uses have been widely recognized in the literature (e.g. Quine et al., 1994; Schoorl et al., 2004; Navas et al., 2007).

Along the study transect, the mean mass activity ^{137}Cs and $^{210}Pb_{ex}$ decreases downslope, and the Anova test indicates that statistically significant differences only existed between the mean activities for the upper slope and bottom slope for $^{210}Pb_{ex}$ (Table 1). The largest variability of ^{137}Cs and $^{210}Pb_{ex}$ mass activity was found at the upper slope and, in general, the variability decreased from the upper to the bottom slope. The mean ^{137}Cs inventories increase from the upper to the midslope and the bottom slope. On the upper slope, the mean of ^{137}Cs inventories was close to the reference inventory, whereas the greatest variability was found on the bottom slope. For $^{210}Pb_{ex}$ the mean inventories were also highest at the bottom of the slope that was also characterized by the largest variability of the inventories. The mean of the inventories was closer to the reference inventory for the upper slope. When compared with the reference inventories for ^{137}Cs and $^{210}Pb_{ex}$ obtained for the study area, ^{137}Cs loss and gain along the transect ranged between 17.8% and 74.0% and between 2.4% and 127.8%, respectively. Similarly, a large variability was found for $^{210}Pb_{ex,}$ with losses ranging between 2.6% and 100.0%, and gains between 20.3% and 246.8%.

As shown in Table 2, the mean values for the various measures of depth distribution of ^{137}Cs showed differences that were tested with Anova between the different parts of the transect. The depth containing 80% of the ^{137}Cs inventory increases along the transect and the mean values for the upper slope and midslope differed significantly from those in the bottom slope. Mixing by tillage of ^{137}Cs in the profiles of the cultivated fields on the bottom slope results in deeper profiles, in which the depth containing 80% of the ^{137}Cs inventory is double that for the profiles from the upper slope. The depth to undetectable ^{137}Cs increases along the transect and on the bottom slope is more than double and significantly different from the upper slope. This pattern is similar to what it was observed along a transect in the Las Bardenas area (Navas and Walling, 1992). Similar trends are observed for $^{210}Pb_{ex}$, as the mean of the depth containing 80% of the $^{210}Pb_{ex}$ in the bottom slope is significantly different from that in the upper slope. The depth to undetectable $^{210}Pb_{ex}$ increased from the upper slope to the bottom slope, reflecting the influence of tillage although differences were not significant.

Considering all the depth intervals separately for the uncultivated and the cultivated soils (Fig. 2), the box plots of the depth distribution of ^{137}Cs and $^{210}Pb_{ex}$ follow the normal pattern for the respective land uses although that of $^{210}Pb_{ex}$ shows higher variability. As expected, ^{137}Cs and $^{210}Pb_{ex}$ were positively and significantly related. Although the correlation was only moderate ($r = 0.451$) it demonstrates the similar behaviour of the two radionuclides once they become attached to the fine soil fraction.

The soil properties show different behaviour along the transect. Stoniness and the sand and organic matter content decrease from the upper slope to the bottom slope whereas the opposite trend is shown by the clay content. The Anova test indicate that mean clay contents in the upper part of the transect differed significantly from those in the midslope and bottom slope whereas the opposite was found for stoniness and mean contents of organic matter were significantly different for the three parts of the slope. (Table 3). This spatial pattern reflects in part the different soil types developed on the diverse lithologies but is mainly a reflection of the impact of land use associated with the occurrence of cultivated fields at the bottom of the slope, which accounts for the low organic matter content and stoniness.

The ^{137}Cs and $^{210}Pb_{ex}$ mass activities were not significantly correlated with clay content, but were significantly and positively correlated with organic matter content, reflecting the higher organic matter content in the upper soil layers that generally coincide with the highest activity of these radionuclides (Table 4). The lack of correlation with clay appears to be related to the fairly uniform depth distribution of clay content in the soil profiles and the absence of any clear decrease with depth as shown by the organic matter for uncultivated soils. Another reason could be the limited range of clay contents.

Estimates of soil redistribution (Mg ha^{-1} $year^{-1}$) derived from the ^{137}Cs inventories, using models reported by Soto and Navas (2004,2008), documented along the transect show that erosion rates range between 2.6 and 31.9 Mg ha^{-1} $year^{-1}$ and sedimentation rates range between 0.2 and 24.5 Mg ha^{-1} $year^{-1}$ (Fig. 3). The magnitude and variation of the ^{137}Cs inventories, and thus the soil redistribution rates recorded along the transect appear to be related to the different land use, slope gradient and soil properties that were distinguished on the three main parts of the transect.

In the upper part of the transect, the natural forest is dense and, in spite of the presence of the steepest slopes (24%), little soil redistribution occurs. Deviations from the reference inventory are within the range of uncertainty for 4 of the 9 sampling points. The sedimentation rates are low (mean 1.8 (±1.5) Mg ha^{-1} $year^{-1}$), and at three points range between 2.9 and 4.0 Mg ha^{-1} $year^{-1}$. Erosion occurs at point 6, an old abandoned field (-3.2 Mg ha^{-1} $year^{-1}$), and at point 8, where, in accordance with field observations, it reaches -19.2 Mg ha^{-1} $year^{-1}$ because of the increased slope.

On the midslope (21% slope), areas with both cultivated and abandoned fields are interspersed with patches of natural forest and the slope shape is highly variable, with relatively flat terraced fields alternating with regular straight slopes. As a result, the magnitude of soil redistribution within this part of the transect varies considerably and both erosion and deposition occur in equal proportions. High erosion rates were found for cultivated points 12, 14, 15 (-14.6, -15.1, -31.9 Mg ha^{-1} year^{-1}, respectively) but a much lower erosion rate of only -2.6 Mg ha^{-1} year^{-1} was found for a sampling point within an abandoned field (point 18). Stable conditions were found at point 10 (old abandoned field) and point 11 under forest. Within the lower part of this section of the transect, deposition occurred at points 16 and 17 (6.3 and 12.8 Mg ha^{-1} year^{-1}, respectively) coinciding with an inflexion of the slope.

The bottom slope, which represents the gentler part of the transect (15% slope), is cultivated for cereals. In this section the largest variability of soil redistribution rates was found. The highest sedimentation rates (24.5, 7.1 and 17.3, Mg ha^{-1} year^{-1}) were recorded for points 20, 21 and 23, respectively, whereas points 19 and 22 suffered relatively high erosion rates (-12.1 and -17.2 Mg ha^{-1} year^{-1}). Therefore, as found in other studies (Quine et al., 1994), cultivation appears to exert a key influence on soil redistribution, causing high soil redistribution rates within this portion of the transect, in spite of the lower slope gradient. Furthermore, in the study area storm events are more frequent after the harvest when the soil surface is left bare (López-Vicente et al., 2008) thus contributing to increase soil redistribution.

The soil redistribution estimates based on ^{137}Cs are consistent with the physiography and the land use along the transect. On the upper slope, little soil movement occurred as indicated by the low rates of erosion and deposition derived from inventories close to the range of uncertainty/stability, suggesting that the presence of dense forest protects the soil surface very effectively. The highest soil losses occur within the cultivated fields of the midslope and the highest deposition rates are found on the bottom slope of the transect that terminates at point 24 which is characterized by the depth distribution to be expected of a lake deposit, as indicated by the presence of the 1963 ^{137}Cs peak at a depth of 45 cm.

The magnitude and variation of the $^{210}Pb_{ex}$ inventories along the transect is greater than that of the ^{137}Cs inventories and therefore the soil redistribution rates estimated using $^{210}Pb_{ex}$ measurements show greater variability, especially on the bottom slope (Fig. 3). Larger variability in $^{210}Pb_{ex}$ inventories compared to ^{137}Cs inventories has also been documented by Mabit et al. (2009) and Porto et al. (2009) and this could also be related with accuracy of gamma measurements of $^{210}Pb_{ex}$ (Shakhashiro and Mabit, 2009) especially for soils with low ^{210}Pb activities as in highly eroded sites or in tilled profiles. On the upper part of the transect both erosion and deposition occurred, but rates were low. The $^{210}Pb_{ex}$ inventories were also close to the reference inventory and erosion was only evident at point 4 (-4.2 Mg ha^{-1} year^{-1}). Little deposition occurred at the bottom of this section and rates were around 2.2 Mg ha^{-1} year^{-1}. Low rates of soil erosion was found for the uncultivated soil profiles associated with the upper and lower parts of the midslope (points 10, 11 and 16), which, based on the ^{137}Cs profiles, provided evidence of low rates of deposition, although values were quite close to stability at points 10 and 11. These discrepancies can be included within the range of uncertainty around stability indicated by the reference inventories of the radiotracers. The land at points 12, 14 and 15 was first abandoned and then cultivated more recently under the European Agrarian Policy. The land use changes that affected this section of the transect during the 20th century introduce problems for the use of $^{210}Pb_{ex}$ measurements to estimate soil redistribution rates, since these profiles do not meet the required steady state conditions for a period of ca. 100 years (Walling and He, 1999; Zhang et al. 2006).

On the bottom slope, the inventories of both ^{137}Cs and $^{210}Pb_{ex}$ for the profiles indicate similar patterns of soil redistribution over the different time periods, but the absolute magnitude of the rates of erosion and deposition estimated for each point differ. Consequently, some points are seen to experience greater rates of erosion and deposition, over the medium-term, as compared to the longer-term as for points 19 and 20, respectively; and vice versa at points 21 and 23 for deposition and 22 for erosion. Deposition based on $^{210}Pb_{ex}$ reached a maximum of 110 Mg ha^{-1} year^{-1} for point 23 which is close to the lake, this value deviates greatly from the ^{137}Cs estimate (17.3 Mg ha^{-1} year^{-1}). High deposition was also found at point 21 (48 Mg ha^{-1} year^{-1}) which is located above a steep bank that separates the field from the pathway and this might help to account for the distinctive processes of soil movement for the different time-periods. Important soil movement that could have been associated with the transformation to agricultural land during the transition between the 19th and 20th centuries on the midslope area, generated substantial amounts of sediment that accumulated in the area close to the steep bank. Furthermore, after the process of land abandonment during the 20th century the collapse of some portions of the terraces due to lack of maintenance may have supplied additional sediment to the lower parts of the slope. After the period of ^{137}Cs fallout, this area still functioned as an accumulation site but rates are not as great. Within the time scale of ^{137}Cs the main changes in land use involving the change to intensive agricultural use at the beginning of the 20th century and the subsequent abandonment and collapse of the agricultural terraces during the last part of the past century would not have affected the contemporary ^{137}Cs inventories as much as it would had affected the $^{210}Pb_{ex}$ inventories. The highest rate of erosion on the transect (-83.7 Mg ha^{-1} year^{-1}) was also found at the bottom of the slope at point 22 that is located below the pathway. The consistency of the pattern of soil movement demonstrated by both radiotracers is evidenced by the high rate of accumulation found at point 23 and also at point 24.

In general, there is reasonable agreement in the evidence for the soil redistribution occurring along the transect during the two different time periods. Means of soil deposition estimates from both ^{137}Cs and $^{210}Pb_{ex}$ measurements and of soil erosion from $^{210}Pb_{ex}$ measurements were much higher and significantly different on the bottom slope than those in the upper and mislope parts of the transect. However, the magnitude of erosion and deposition differed between the estimates derived from the ^{137}Cs and $^{210}Pb_{ex}$ measurements (Table 5). Walling et al. (2003) and Zhang et al. (2006) recognized that the two radionuclides are unlikely to provide identical results, due to the different time periods involved. This can be especially relevant in areas, such as the study area, that have been affected by important land use changes occurring during different periods but differences in rainfall intensity over the two different periods may also have had an effect.

The rates of soil redistribution based on $^{210}Pb_{ex}$ estimates are in general lower than those based on ^{137}Cs, especially at the upper and middle parts of the transect. However, the contrary was observed in sites of the lower slope where high sediment accumulation could reflect increased soil erosion and sediment supply that may have occurred during the 20th century due to the collapse of some of the terraces after land abandonment. Porto et al. (2009) found that soil redistribution rates from $^{210}Pb_{ex}$ were higher than those derived from ^{137}Cs measurements and these differences were interpreted as being a result of the different temporal sensitivity of the two radionuclides to ongoing soil redistribution. Zhang et al. (2006) recognized that although $^{210}Pb_{ex}$ measurements will reflect the erosional history over a longer time period, the shorter half-life and the continuous fallout mean that $^{210}Pb_{ex}$ inventories are also likely to be more sensitive to recent changes in erosional activity than ^{137}Cs.

Over the time-scale reflected by the ^{137}Cs measurements, higher intensity soil erosion occurred especially at the midslope as a consequence of the process of land abandonment in the middle part of the past century that was followed by increased accumulation of sediment on the bottom slope, although erosion was here less intense. The relationship between the soil redistribution rates derived from ^{137}Cs and $^{210}Pb_{ex}$ measurements shows a statistically significant positive relationship (r = 0.596) between both estimates, which, although of only moderate significance, indicates similarity in the overall pattern of soil redistribution over the past 100 years. Walling et al. (2003) also found a clear positive relationship between the soil redistribution rates derived for the longer- ($^{210}Pb_{ex}$ - ca. 100 years) and medium-term (^{137}Cs - ca. 50 years) time scales. However, the greater deviations found in our study may be due to greater changes in the intensity of processes through time, which are in turn related to important land use changes. Several studies in Northern Spain (e.g. Navas et al., 2009) have confirmed that in the first part of the 20th century the intensity and frequency of floods were particularly high due to increased runoff from cultivated fields, because of the large surface area covered by agricultural land in this period.

Estimates of soil redistribution based on ^{7}Be measurements undertaken along a parallel transect on the same slope for an individual storm event of 22 mm in 2007 (Navas et al., 2008) indicated that apart from one, all points suffered erosion and that the highest rate occurred on the upper part of the transect and the lowest at the bottom slope. These results highlight the complexity of the soil redistribution process and emphasise the need to consider a range of factors, including land use, topography and rainfall intensity, when interpreting changing patterns of soil movement in space and time. The influence of temporal scale on soil redistribution estimates will reflect many factors, particularly the changes in land use and rainfall characteristics (López-Moreno et al., 2009) that have occurred during the past century in the study area and that need further exploration.

4. Conclusions

The deviation of the measured ^{137}Cs and $^{210}Pb_{ex}$ inventories from the reference inventories and the associated estimates of soil redistribution rates indicated that within the upper part of the transect investigated in this study, with an average slope gradient of 24%, soil stability predominated under forest. On the midslope portion of the transect (21% slope), which is characterized by a great variety of land use and vegetation cover, erosion predominates but deposition also occurs. On the bottom slope of the transect (15% slope), where cultivation is the main land use, both radionuclides indicated high sediment deposition but also significant erosion was found immediately below a pathway, reflecting the impact of agricultural land use on the pattern of soil mobilization.

The different magnitude and patterns of soil movement along the transect documented by both radionuclides demonstrate that both land use and slope gradient exert important controls on soil redistribution rates. For steep slopes the dense forest on the upper part of the transect protects the soil surface from erosion.

The estimates of soil loss obtained from the ^{7}Be measurements suggested that soil loss predominated along most of the transect. However, over the longer temporal scale provided by the ^{137}Cs and $^{210}Pb_{ex}$ measurements, a different spatial pattern of soil redistribution, that more closely reflects the topography and land use along the transect were documented.

This research demonstrates the potential for coupling $^{210}Pb_{ex}$ and ^{137}Cs measurements for assessing soil redistribution in Mediterranean environments at different temporal scales and provides evidence of the complex patterns of erosion and deposition that exist in the landscape. Uncertainties associated with the application of $^{210}Pb_{ex}$ in highly heterogeneous environments, such as found in Mediterranean mountains, need to be investigated further to improve the accuracy of estimates of soil redistribution provided by $^{210}Pb_{ex}$ measurements, by better defining the appropriate depth increment for core sectioning, as a function of land use.

Acknowledgments

This work was funded by the CICYT project MEDEROCAR (CGL2008-0831).

References

Crickmore, M.J., Tazioli, G.S., Appleby, P.G., Oldfield, F., 1990. The use of nuclear techniques in sediment transport and sedimentation problems. UNESCO Technical Documents in Hydrology, UNESCO, Paris.

CSIC. 1976. Comisión de métodos analíticos. Anales Edafol. Agrobiol., 35: 813-814.

Ferrero, J.L., Jorda, M.L., Milio,J., Monforte, L., Moreno, A. Navarro, E., Senent, F., Soriano, A., Baeza, A., del rio, M., 1987. Atmospheric radioactivity in Valencia, Spain, due to the Chernobyl reactor accident. Health Physics, 53 (5): 519-524.

He, Q., Walling, D.E., 1997. The distribution of fallout ^{137}Cs and ^{210}Pb in undisturbed and cultivated soils. Applied Radiation and Isotopes, 48: 677-690.

Kato, H., Onda, Y., Tanaka. Y., 2010. Using ^{137}Cs and $^{210}Pb_{ex}$ measurements to estimate soil redistribution rates on semi-arid grassland in Mongolia. Geomorphology, 114: 508-519.

Liu, H., Jacob, D.J., Bey, I., Yantosca, R.M., 2001. Constraints from Pb-210 and Be-7 on wet deposition and transport in a global three-dimensional chemical tracer model driven by assimilated meteorological fields. Journal of Geophysical Research (Atmospheres), 106 (D11): 12109-12128.

López-Moreno J.I., Vicente-Serrano S., Beguería S., Angulo-Martínez M., 2009. Trends in daily precipitation (1955-2006) over north-eastern Iberian Peninsula. International Journal of Climatology. doi: 10.1002/joc.1945.

López-Vicente, M., Navas, A., Machín, J., 2008. Identifying erosive periods by using RUSLE factors in mountain fields of the Central Spanish Pyrenees. Hydrology and Earth System Sciences, 12: 523–535.

Mabit, L., Benmansour, M., Walling, D.E., 2008. Comparative advantages and limitations of fallout radionuclides (^{137}Cs, ^{210}Pb and ^{7}Be) to assess soil erosion and sedimentation. Journal of Environmental Radioactivity, 99 (12): 1799–1807.

Mabit, L. Klik, A., Benmansour, M., Toloza, A., Geisler, A., Gerstmann, U.C., 2009. Assessment of erosion and deposition rates within an Austrian agricultural watershed by combining ^{137}Cs, $^{210}Pb_{ex}$ and conventional measurements. Geoderma, 150: 231-239.

Matisoff, G., Bonniwell, E.C., Whiting, P.J., 2002. Soil erosion and sediment sources in an Ohio Watershed using Beryllium-7, Cesium-137, and Lead-210. Journal Environment Quality, 31: 54-61.

Meehl, G.A., W.M. Washington, W.D. Collins, J.M. Arblaster, A. Hu, L.E. Buja, W. G. Strand and H. Teng., 2005. How much more global warming and sea level rise. Science, 307: 1769-1772.

Molero, J., Sanchez-Cabeza, J.A., Merino, J., Mitchell, P.I., Vidal-Quadras, A., 1999. Impact of ^{134}Cs and ^{137}Cs from the Chernobyl reactor accident on the Spain Mediterranean marine environment. Journal of Environmental Radioactivity, 43: 357-370.

Navas, A., Walling, D.E., 1992. Using caesium-137 to assess sediment movement in a semiarid upland environment in Spain. In: D.E. Walling, T.R., Davies, B. Hasholt, (Editors), Erosion, Debris Flows and Environment in Mountain Regions. Wallingford, IAHS Publ. 209, pp. 129–138.

Navas, A., Machín, J., Soto, J., Valero-Garcés, B.L., 2003. Radiotrazadores de la erosión/sedimentación: aplicaciones en laderas de ambientes mediterráneos. In: R. Bienes, M.J., Marqués (editors). Control de la erosión y degradación del suelo, pp. 577-580.

Navas, A., Machín, J. and Soto, J., 2005. Assessing soil erosion in a Pyrenean mountain catchment using GIS and fallout ^{137}Cs. Agriculture, Ecosystems and Environment, 105: 493-506.

Navas, A., Walling, D.E., Quine, T., Machín, J., Soto, J., Domenech, S. y López-Vicente, M., 2007. Variability in ^{137}Cs inventories and potential climatic and lithological controls in the central Ebro valley, Spain. Journal of Radioanalytical and Nuclear Chemistry, 274: 331-339.

Navas, A., Walling, D.E., Gaspar, L., Machín, J., 2008. Use of Beryllium-7 to assess soil redistribution by erosion in two contrasting Mediterranean environments. In: J. Schmidt, T. Cochrane, C. Phillips, S. Elliott, T. Davies, L. Basher (editors), Sediment Dynamics in Changing Environments. IAHS Publ. 325, pp. 43-51.

Navas, A., Valero-Garcés, B.L, Gaspar, L., Machín, J., 2009. Reconstructing the history of sediment accumulation in the Yesa reservoir: an approach for management of mountain reservoirs. Lake and Reservoir Management, 25 (1): 15-27.

Porto, P., Walling, d.E., Gallegari, G., Catona, F., 2006. Using fallout Lead-210 measurements to estimate soil erosion in three small catchments in southern Italy. Water, Air, and Soil Pollution, 6: 657-667.

Porto, P., Walling, D.E., Callegari, G., Capra, A., 2009. Using caesium-137 and unsupported lead-210 measurements to explore the relationship between sediment mobilisation, sediment delivery and sediment yield for a Calabrian catchment. Marine & Freshwater Research, 60 (7): 680-689.

Quine, T., Navas, A., Walling, D.E., Machín, J., 1994. Soil erosion and redistribution on cultivated and uncultivated land near Las Bardenas in the Central Ebro River Basin, Spain. Land Degradation and Rehabilitation, 5: 41–55.

Ritchie, J.C., Ritchie, C.A., 2007. Bibliography of publications of ^{137}Cs studies related to erosion and sediment deposition. http://www.ars.usda.gov/Main/docs.htm?docid¼15237.

Sadiki, A., Faleh, A., Navas, A., Bouhlassa, S. 2007. Assessing soil erosion and control factors by the radiometric technique in the Boussouab catchment, Eastern Rif, Morocco. Catena, 71 (1): 13-20.

Sanchez-Cabeza, J.A., Garcia-Talavera, M., Costa, E., Peña, V., Garcia-Orellana, J., Masqué, P., Nalda, C., 2007. Regional calibration of erosion radiotracers (^{210}Pb and ^{137}Cs): Atmospheric fluxes to soils (Northern Spain). Environmental Science & Technology, 41: 1324-1330.

Shakhashiro, A., Mabit, L., 2009. Results of an IAEA inter-comparison exercise to assess ^{137}Cs and total ^{210}Pb analytical performance in soil. Applied Radiation and Isotopes, 67 (1): 139–146.

Schoorl, J.M., Boix Fayos, C., de Meijer, R.J., van der Graaf, E.R., Veldkmp, A., 2004. The ^{137}Cs technique applied to steep Mediterranean slopes (Part I): the effects of lithology, slope morphology and land use. Catena, 57: 15-34.

Schuller, P, Iroumé, A., Walling, D. E., Mancilla, H. B., Castillo, A., Trumper, R. E., 2006. Use of beryllium-7 to document soil redistribution following forest harvest operations. Journal of Environmental Quality, 35: 1756-1763.

Soto, J., Navas, A., 2004. A model of ^{137}Cs activity profile for soil erosion studies in uncultivated soils of Mediterranean environments. Journal of Arid Environments, 59: 719-730.

Soto, J., Navas, A., 2008. A simple model of Cs-137 profile to estimate soil redistribution in cultivated stony soils. Radiation Measurements, 43: 1285-1293.

Verheijen, F.G.A., Jones, R.J.A., Rickson, R.J., Smith, C.J., 2009. Tolerable versus actual soil erosion rates in Europe. Earth-Science Reviews, 94: 23-38.

Wallbrink, P.J., Murray, A.S., 1996. Determining soil loss using the inventory ratio of excess Lead-210 to Cesium-137. Soil Science Society of America Journal, 60: 1201-1208.

Walling, D.E., Quine, T.A., 1990. Calibration of caesium-137 measurements to provide quantitative erosion rate data. Land Degrad. Rehabil, 2: 161-175.

Walling, D.E., He, Q. y Quine, T.A., 1995. Use of caesium-137 and lead-210 as tracers in soil erosion investigations. IAHS Publ. 229, pp 163-172.

Walling, D.E., He, Q., 1999. Using fallout lead-210 measurements to estimate soil erosion on cultivated land. Soil Science Society of America Journal, 63: 1404–1412.

Walling, D.E., He, Q., Blake, W., 1999. Use of ^{7}Be and ^{137}Cs measurements to document short- and medium-term rates of water-induced soil erosion on agricultural land. Water Resources Research, 35: 3865-3874.

Walling, D.E., Collins, A.L. y Sichingabula, H.M., 2003. Using unsupported lead-210 measurements to investigate soil erosion and sediment delivery in a small Zambian catchment. Geomorphology, 52: 193-213.

Zapata, F. (Ed.), 2002. Handbook for the Assessment of Soil Erosion and Sedimentation using Environmental Radionuclides. Kluwer Ac. Publ., Dordrecht, The Netherlands, pp. 219.

Zhang, X., Qi, Y., Walling, D.E., He, X., Wen, A. y Fu, J., 2006. A preliminary assessment of the potential for using $^{210}Pb_{ex}$ measurement to estimate soil redistribution rates on cultivated slopes in the Sichuan Hilly basin of China. Catena, 68 : 1-9.

Tables

Table 1. Summary statistics of ^{137}Cs and $^{210}Pb_{ex}$ mass activities and inventories in the soil profiles for the whole transect and for the different parts of the transect.

	^{137}Cs	^{137}Cs	$^{210}Pb_{ex}$	$^{210}Pb_{ex}$
	Bq kg^{-1}	Bq m^{-2}	Bq kg^{-1}	Bq m^{-2}
total transect n=23				
mean	8.1	1812.1	8.4	2049.1
median	5.4	1671.1	7.8	1787.4
standard deviation	8.7	1135.6	9.4	1746.3
standard error	1.8	236.8	2.0	364.1
range	0.8 – 37.9	408.7 – 6080.1	0.0 – 41.3	0.0 – 6734.4
upper slope n=9				
mean	12.6	1650.3	13.8	1890.7
median	8.0	1688.9	8.9	2335.6
standard deviation	11.9	505.6	12.9	948.6
standard error	4.0	168.5	4.3	316.2
range	2.4 – 37.9	671.6 – 2455.6	0.0 – 41.3	0.0 – 3019.2
midslope n=8				
mean	5.9	1682.3	5.5	1783.2
median	6.4	1420.5	4.8	1534.8
standard deviation	3.2	881.4	3.6	1646.3
standard error	1.1	311.6	1.3	582.0
range	2.2 – 10.0	829.8 – 3575.9	0.0 – 10.2	0.0 – 4941.9
bottom slope n=6				
mean	4.1	2228.1	4.0	2641.1
median	2.5	1776.3	3.8	1936.0
standard deviation	5.0	1973.9	3.6	2757.6
standard error	2.0	805.8	1.5	1125.8
range	0.8 – 14.1	408.7 – 6080.1	0.0 – 8.4	0.0 – 6734.4

Table 2. Average values of the total ^{137}Cs and $^{210}Pb_{ex}$ inventories, depth containing 80% of ^{137}Cs and $^{210}Pb_{ex}$ inventories and depth to undetectable ^{137}Cs and $^{210}Pb_{ex}$ inventories in the three parts of the transect.

	^{137}Cs Bq m^{-2}	^{137}Cs depth containing 80% cm	depth to zero cm	$^{210}Pb_{ex}$ Bq m^{-2}	$^{210}Pb_{ex}$ depth containing 80% cm	depth to zero cm
upper slope	1650.3 (±505.6) a	13 (±5.6) a	16 (±5.5) a	1890.7 (±948.6) a	13 (±9.1) a	19 (±14.7) a
midslope	1682.3 (±881.4) a	16 (±6.8) a	26 (±12.1) a	1783.2 (±1646.3) a	14 (±9.9) ab	25 (±14.9) a
bottom slope	2228.1 (±1973.9) a	29 (±10.7) b	36 (±8.0) b	2641.1 (±2757.6) a	28 (±18.1) b	34 (±20.1) a

Different letters indicate significant differences at the p-level <0.05

Table 3. Summary statistics for the physico-chemical soil properties in the sample intervals along the transect and for the different parts of the transect.

	organic matter %	clay %	silt %	sand %	stone content %
total n=143					
mean	3.2	24.5	69.0	6.5	27.9
median	2.3	23.9	73.4	0.2	25.6
standard deviation	2.4	10.7	13.7	15.2	21.1
standard error	0.2	0.9	1.1	1.3	1.8
range	0.2 – 12.9	0.6 – 83.4	14.4 – 84.9	0.0 – 85.0	0.0 – 76.2
upper slope n=38					
mean	4.8	20.8	63.6	15.6	33.7
median	4.5	19.4	72.4	3.9	31.0
standard deviation	2.5	11.8	18.2	22.0	20.3
standard error	0.4	1.9	3.0	3.6	3.3
range	1.0 – 12.9	4.3 – 77.9	17.3 – 84.9	0 – 76.3	3.4 – 76.2
midslope n=47					
mean	3.7	25.7	71.1	3.2	40.0
median	3.2	24.9	73.1	0.1	39.7
standard deviation	2.6	6.6	7.5	8.3	19.4
standard error	0.4	1.0	1.1	1.2	2.8
range	0.5 – 12.3	12.0 – 48.0	42.4 – 83.2	0 – 45.6	4.1 – 68.2
bottom slope n=58					
mean	1.7	26.0	70.8	3.1	14.4
median	1.6	24.1	73.6	0.1	11.5
standard deviation	1.2	12.2	13.3	11.6	14.4
standard error	0.2	1.6	1.7	1.5	1.9
range	0.2 – 7.8	0.6 – 83.4	14.4 – 81.3	0 – 85.0	0 – 55.8

Table 4. Pearson correlation coefficients between ^{137}Cs and $^{210}Pb_{ex}$ inventories and soil properties for the sample intervals along the transect and for the different parts of the transect.

	total n=143		upper slope n=38		midslope n=47		bottom slope n=58	
	^{137}Cs	$^{210}Pb_{ex}$	^{137}Cs	$^{210}Pb_{ex}$	^{137}Cs	$^{210}Pb_{ex}$	^{137}Cs	$^{210}Pb_{ex}$
clay	**-0.17**	0.01	-0.26	0.03	**-0.41**	0.08	-0.00	0.03
organic matter	**0.50**	**0.32**	**0.70**	**0.60**	**0.36**	0.01	**0.67**	0.22
stone	-0.07	-0.02	-0.01	0.18	-0.20	**-0.35**	-0.22	-0.13
silt	0.01	-0.05	0.02	-0.09	0.02	0.04	0.07	0.06
sand	0.11	0.04	0.12	0.05	**0.30**	-0.10	-0.07	-0.10

Bold face numbers significant at the 95% confidence level

Table 5. Mean values of ^{137}Cs and $^{210}Pb_{ex}$ soil redistribution rates and values of standard deviation in the three parts of the transect.

	^{137}Cs		$^{210}Pb_{ex}$	
	erosion	deposition	erosion	deposition
	Mg ha^{-1} year^{-1}	Mg ha^{-1} year^{-1}	Mg ha^{-1} year^{-1}	Mg ha^{-1} year^{-1}
upper slope	11.2 ±11.3 a	1.8 ±1.5 a	1.7 ±1.8 a	1.3 ±0.6 a
midslope	16.1 ±12.0 a	5.1 ±5.8 a	2.2 ±1.7 a	-
bottom slope	14.7 ±3.6 a	16.3 ±8.7 b	44.0 ±56.2 b	57.1 ±49.0 b
total transect	14.5 ±9.3	5.9 ±7.4	9.6 ±24.6	22.2 ±39.0

Different letters indicate significant differences at the p-level <0.05

Figures

Fig. 1. The study area, showing its location, the position of the sampling points along the transect and the geology, land use and soil types associated with the upper slope, midslope and bottom slope portions of the transect.

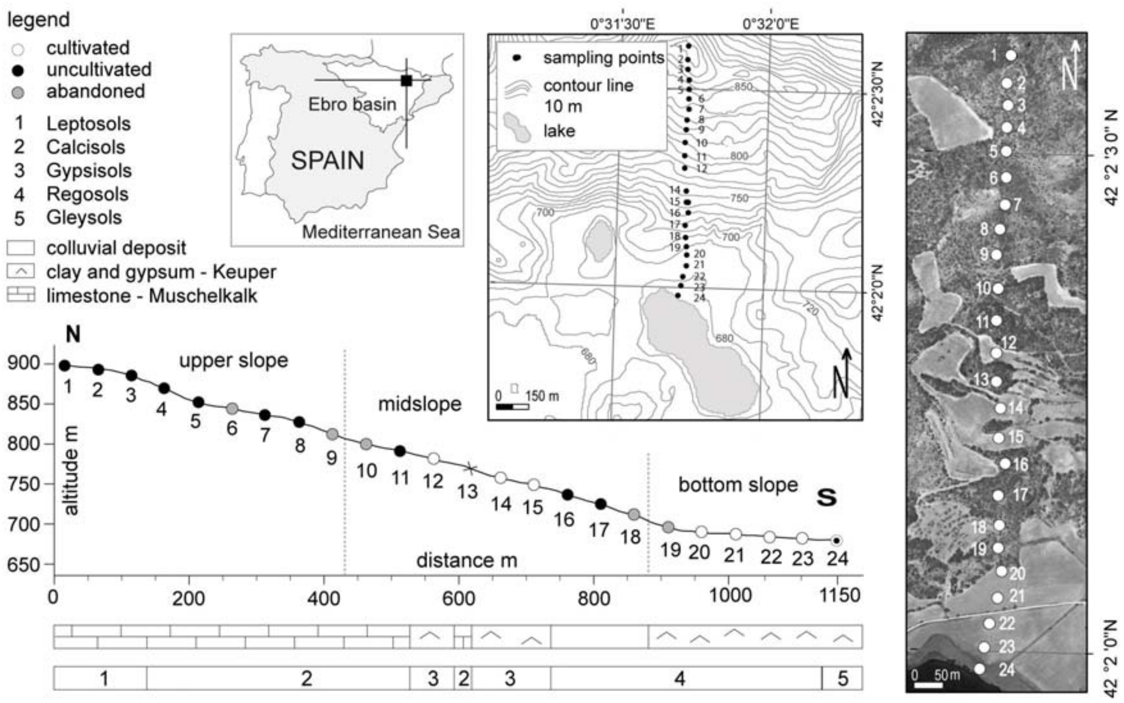

Fig. 2. The distribution of $^{210}Pb_{ex}$ and ^{137}Cs mass activities and inventories in uncultivated and cultivated soils.

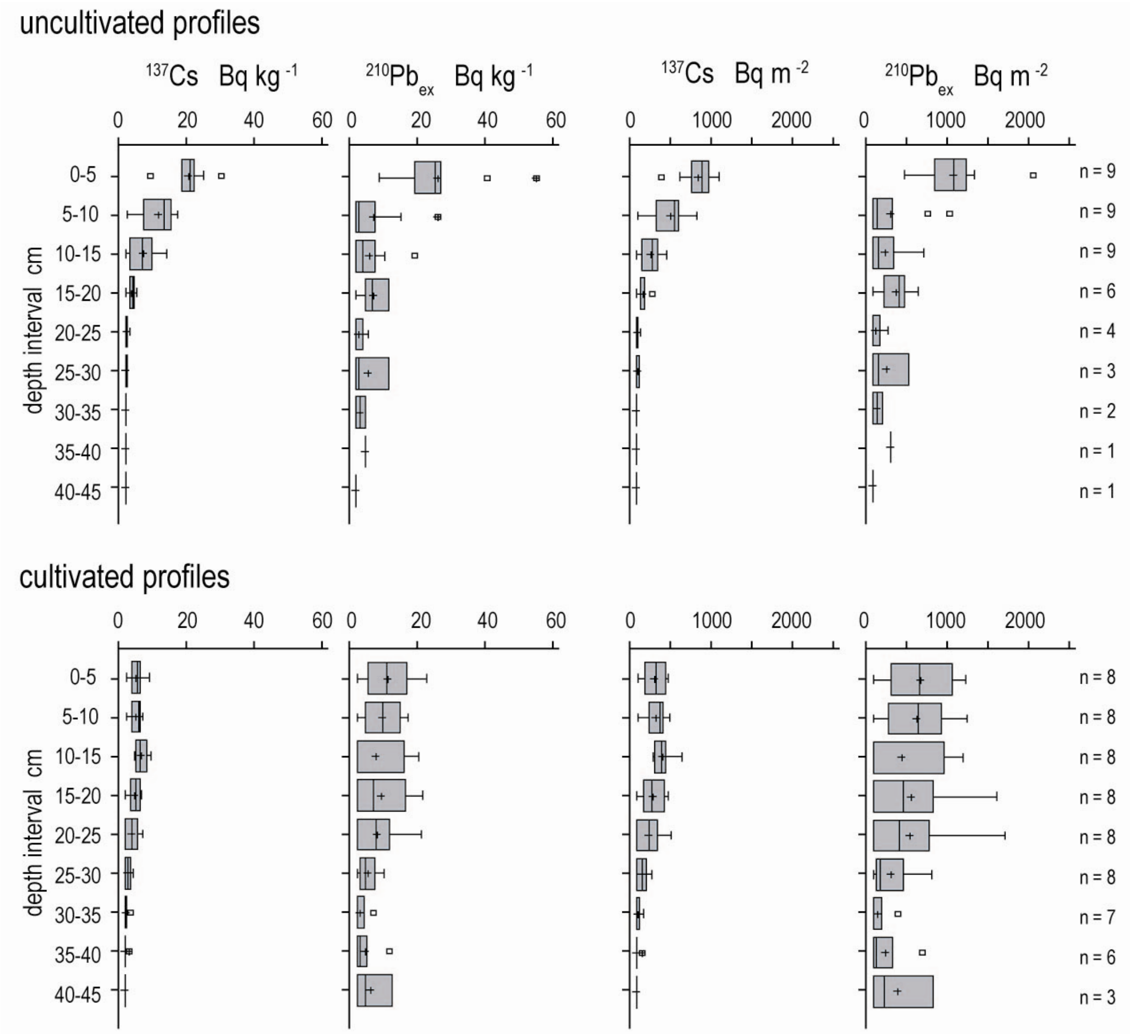

Fig. 3. Estimates of soil redistribution rates and errors for the individual sampling points along the transect based on the $^{210}Pb_{ex}$ and ^{137}Cs measurements.